International Journal of Nanoelectronics and Materials
Volume 16 (Special Issue) December 2023 [1-8]

Effects of Iron Doped $LiTaO_3$ Films on Transverse Optic (TO) and Longitudinal Optic (LO) Values Using Kramers-Kronig Method

Irzaman[1,*], Syahrul[1], Nazopatul Patonah Har[1], Teguh Puja Negara[1,2], Irmansyah[1], and Husin Alatas[1]

[1]Department of Physics, Faculty of Mathematics and Natural Sciences, IPB University, Bogor 16680, Indonesia
[2]Department of Computer Science, Faculty of Mathematics and Natural Sciences, Pakuan University, Bogor

ABSTRACT

Film fabrication of $LiTaO_3$ has been successfully prepared with 0%, 2%, 4%, and 6% Iron containing variations using the Chemical Solution Deposition (CSD) method. Each sample was characterized using FTIR and the wavenumber and transmittance values were obtained. This value was analyzed using the Kramers-Kronig (KK) method and obtained the Transverse Optic (TO) and Longitudinal Optic (LO) values. The results show that TO value is in wave numbers 462.25 cm^{-1} – 556.00 cm^{-1}. While the value of LO is in the range of wave numbers 478.50 cm^{-1} – 571,00 cm^{-1}. The results show an increase in both TO and LO values as the Iron Oxide percentage increases. Based on the analyses of TO, LO, ε_1 and ε_2, film fabrication of $LiTaO_3$ has the potential as light, pressure and temperature sensors.

Keywords: $LiTaO_3$ Film, Iron doped, Transverse Optic, Longitudinal Optic, Kramers-Kronig

1. INTRODUCTION

Research on semiconductor ferroelectric materials has garnered significant attention from physicists. This is due to the high potential of these materials for advancing new generation devices, given their unique properties [1]. Furthermore, driven by their wide-ranging applicability, ferroelectric materials have captured the interest of researchers. Applications of ferroelectric materials include capacitors, transducers, switches, memory devices, and sensors [2][3][4].

Previous researchers have developed both $LiTaO_3$ films and bulk $LiTaO_3$ materials, characterizing them to establish their potential as ferroelectrics [5]. $LiTaO_3$ is a non-hygroscopic crystal, preserving its optical properties and making it superior to other materials [6].

$LiTaO_3$ films can be produced through various methods, including Pulsed Laser Deposition (PLD) [7], Metal Organic Solution Deposition (MOSD), Sol-Gel Process, and RF Magnetron Sputtering [8]. However, these three methods are relatively costly. Alternatively, the Chemical Solution Deposition (CSD) method, developed since the 1980s for growing perovskite thin films, can be employed [9].

In this study, $LiTaO_3$ films will be fabricated using the Chemical Solution Deposition (CSD) method with a lithium tantalate ($LiTaO_3$) sol-gel on a silicon p-type (100) substrate. The spin coating technique at a rotational speed of 8000 rpm will be used, with varying percentages of the material's dopant Iron (0%, 2%, 4%, 6%). This method offers several advantages, including its feasibility in a simple laboratory setup without vacuum requirements and its cost- effectiveness.

* Corresponding authors: irzaman@apps.ipb.ac.id

This paper addresses the analysis of the influence of Iron Oxide doping (0%, 2%, 4%, 6%) within thin $LiTaO_3$ films on TO and LO values using the Kramers-Kronig method.

2. MATERIAL AND METHOD

The materials utilized in this research consist of lithium acetate $Li(CH_3COO)$ powder 99.6%, Tantalum Oxide (Ta_2O_5) 99.9%, Iron Oxide dopant (Fe_2O_3), ethanol, ethylene glycol, p-type Silicon (100) substrate, and deionized water. The instrument employed for characterization is the Shimadzu Type IR Prestige 21 Fourier Transform Infrared Spectrometer (FTIR).

2.1 Substrate and Solution Preparation

Using a diamond blade knife, the p-type silicon substrate (100) was cut into square pieces measuring 1 cm x 1 cm. Subsequently, the substrate was cleaned with deionized water and dried. In the first stage, 0.3103 grams of Lithium Acetate $Li(CH_3COO)$ powder 99.9% were mixed with 0.9375 ml of acetic acid, stirred with 7 drops of ethanol using a magnetic stirrer set at 800 rpm and a temperature of 60°C for 60 minutes. In the second stage, 1.043 grams of Tantalum Oxide (Ta_2O_5) 99.9% were added to the solution (ethylene glycol and acetic acid) and stirred using a magnetic stirrer at 800 rpm for 60 minutes. In the third stage, 2%, 4%, and 6% of Iron Oxide (Fe_2O_3) were introduced into the solution from the second stage and stirred using a magnetic stirrer at 800 rpm for 60 minutes. In the fourth stage, 0.3125 ml of ethylene glycol and acetic acid were added to the solution from the third stage and stirred using a magnetic stirrer at 800 rpm for 30 minutes, resulting in a $LiTaO_3$ solution with a concentration of 2 M. Table 1 illustrates the chemical composition of the $LiTaO_3$ solution doped with 0%, 2%, 4%, and 6% Iron Oxide (Fe_2O_3).

Table 1 Chemical Composition of Each $LiTaO_3$ Solution

Material	Lithium Acetate (g)	Tantalum Oxide (g)	Acetate Acid (ml)	Ettilene glycol (ml)	$LiTaO_3$ (g)	Iron (g)
$LiTaO_3$+0%Iron	0.3103	1.043	0.9375	0.3125	0.589	0
$LiTaO_3$+2%Iron	0.3103	1.043	0.9375	0.3125	0.589	0.01178
$LiTaO_3$+4%Iron	0.3103	1.043	0.9375	0.3125	0.589	0.02356
$LiTaO_3$+6%Iron	0.3103	1.043	0.9375	0.3125	0.589	0.03534

2.2 Film Growth

Film Growth Using CSD Method on Spin Coater Reactor Surface. The film was grown using the CSD method on the surface of a spin coater reactor. A cleaned p-type Si (100) substrate was placed on the spin coating reactor platter. Half of the p-type Si (100) substrate was treated with 2 drops of the $LiTaO_3$ precursor solution. Then, the spin coater reactor was activated, set to rotate at 8000 rpm for 60 seconds with a 60-second pause interval. This deposition process was repeated three times to obtain three layers on the p-type Si (100) substrate. Following this, the p-type Si (100) substrate was annealed using a furnace at a temperature of 850°C, with a heating rate of 100°C/hour, and held at this temperature for 8 hours [10][11].

2.3 FTIR Characterization Stage

Using FTIR ATR (Attenuated Total Reflectance) spectrophotometer was characterized to examine the optical properties of the thin $LiTaO_3$ film samples before and after doping with Iron Oxide. The obtained values include the wavenumber (ω) and transmittance (T) values of each thin $LiTaO_3$ film.

This test was conducted within the wavenumber range of 400–1500 cm^{-1}. The FTIR data was characterized using the Kramers-Kronig (KK) method, resulting in TO and LO values [12][13]. Figure 1 illustrates the transmission measurement scheme under different conditions (normal and inclined angles) [14].

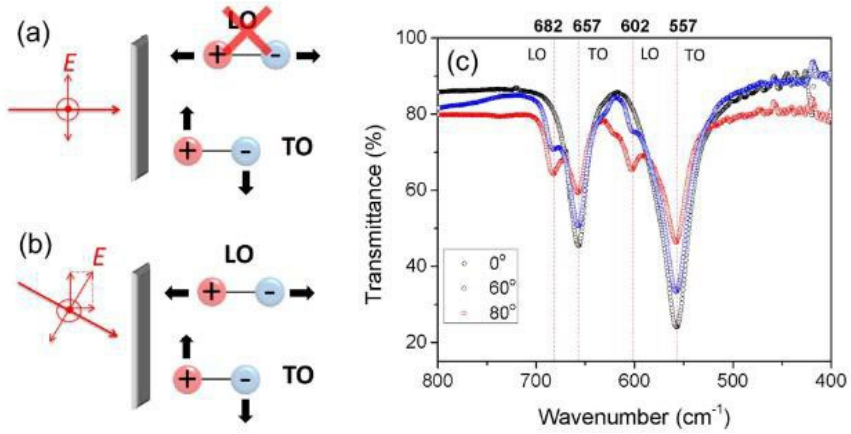

Figure 1. (a-b) Schematic for transmission measurement with (a) normal incidence and (b) oblique incidence. (c) FTIR transmission spectra of Co_3O_4 film on Si with three incident angles of 0°, 60° and 80° [14].

Based on the transmittance values and wavenumber from the FTIR measurement data, the values of TO and LO, as well as the dielectric function values, can be calculated using equations (1) to (7) [12][13][14].

The transmittance value (T) is processed using equations (1) and (2) to obtain the absorbance (A) and reflectance (R) values.

$$A(\omega) = 2 - log[T(\omega)] \quad (1)$$

$$R(\omega) = 100 - [T(\omega)] + A(\omega)] \quad (2)$$

The reflectance value (R) is substituted into equations (3) and (4) to obtain the real refractive index and imaginary refractive index values.

$$n(\omega) = \frac{1-R(\omega)}{1+R(\omega)-2\sqrt{R(\omega)}cos\varphi(\omega)} \quad (3)$$

$$k(\omega) = \frac{2\sin\varphi(\omega)\sqrt{R(\omega)}}{1+R(\omega)-2\sqrt{R(\omega)}cos\varphi(\omega)} \quad (4)$$

Where the phase difference $\varphi(\omega)$ represents the photon reflection after interacting with the sample. The value of $\varphi(\omega)$ is calculated using equation (5).

$$\varphi(\omega) = -\frac{4\omega j}{\pi}\Delta\omega \sum_i \frac{\ln\sqrt{(R(\omega))}}{\omega_i^2-\omega_j^2} \quad (5)$$

Where the index j represents the series of wavenumbers, with the condition that if j is an odd wavenumber value, then index i is an even wavenumber value. Conversely, if i is an odd wavenumber value, then j is an even wavenumber value.

The intersection values of the refractive indices n and k at low wavenumbers are referred to as TO, while the intersections at high wavenumbers are referred to as LO.

The dielectric function value is the square of the refractive index [10]. The values of the real dielectric function (ε_1) and the imaginary dielectric function (ε_2) are calculated using equations (6) and (7).

$$\varepsilon_1 = n^2(\omega) - k^2(\omega) \tag{6}$$

$$\varepsilon_2 = 2n(\omega)k(\omega) \tag{7}$$

3. RESULTS AND DISCUSSION

3.1 Optical Properties of $LiTaO_3$ Film

The results obtained from the characterization using the FTIR instrument consist of wavenumber values and transmittance values, which will be further processed in the subsequent stage to determine the comparison of the influence of the dopant percentage on the $LiTaO_3$ film. The effect of the Iron Oxide dopant percentage on the $LiTaO_3$ film is illustrated in Figure 2.

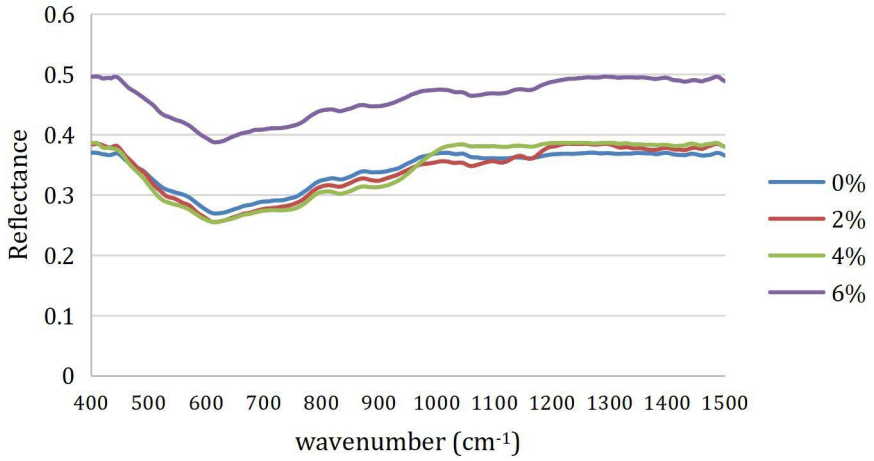

Figure 2. Effect of the percentage of Iron Oxide on the reflectance value of $LiTaO_3$ thin films.

Figure 2 is based on the previous research [13]. Based on Figure 2, it depicts the graph of reflectance values for each percentage of Iron Oxide dopant within the $LiTaO_3$ thin film. A higher percentage of Iron Oxide dopant leads to an increase in the reflectance values.

The transmittance values for each LiTaO3 thin film are processed using the Kronig-Kramers method based on equations (1) to (7) to obtain refractive index values, consisting of the real refractive index (n) and the imaginary refractive index (k). The intersection values of the real and imaginary refractive indices are referred to as TO and LO properties, respectively. The intersection at lower wavenumbers indicates TO property, while LO property is observed at higher wavenumbers. TO and LO values for each $LiTaO_3$ thin film are shown in Figure 3.

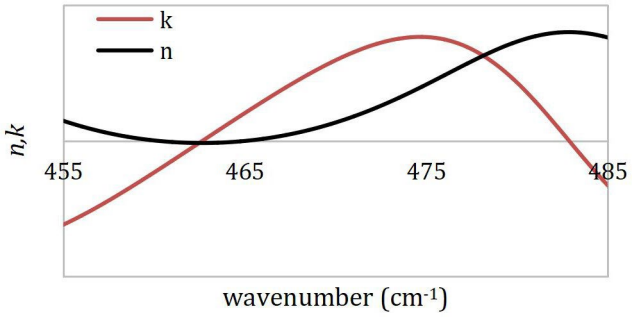

(a)

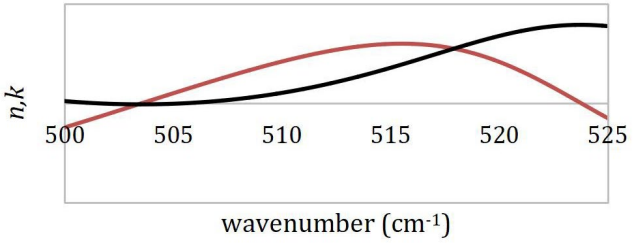

(b)

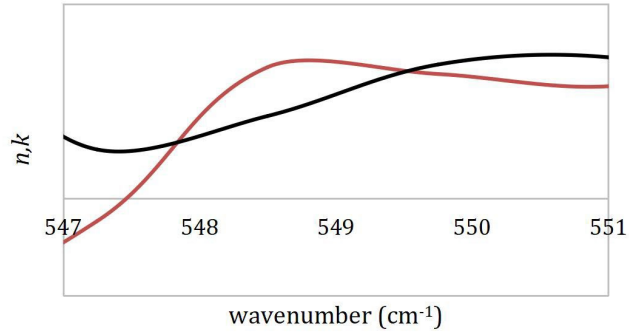

(c)

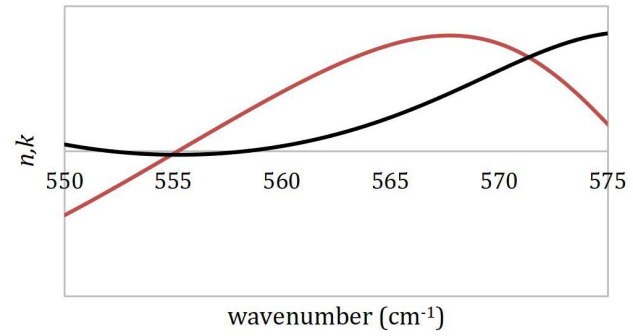

(d)

Figure 3. LO and TO values in the $LiTaO_3$ films doped with Iron Oxide are as follows: (a) 0%, (b) 2%, (c) 4%, and (d) 6%.

Table 2 TO and LO Values of Iron Oxide Doped $LiTaO_3$ Thin Films based on Figure 3

Iron Oxide (%)	TO (cm^{-1})	LO (cm^{-1})	Δ (LO-TO) (cm^{-1})
0	462,25	478,50	16,25
2	503,50	519,75	16,25
4	547,90	551,00	3,10
6	556,00	571,00	15,00

Table 2 shows TO and LO values of Iron Oxide doped $LiTaO_3$ Thin Films based on Figure 3. The larger the percentage of Iron Oxide dopant added to the $LiTaO_3$ thin film, the greater the values of LO and TO. This result is presumed to be due to the increase in reflectance values as shown in Figure 2.

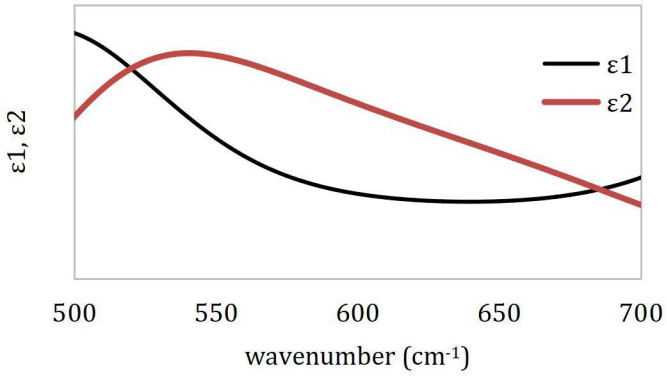

(a)

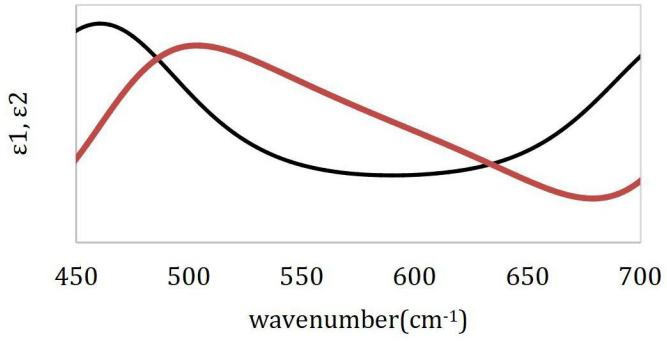

(b)

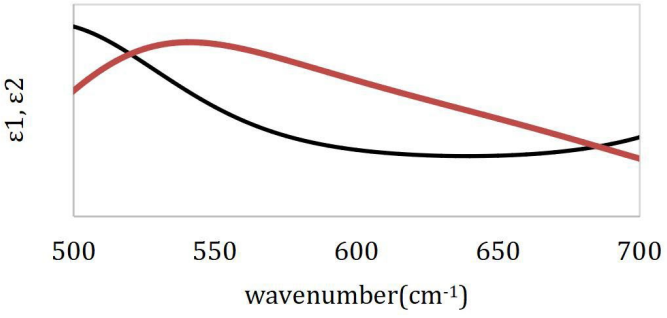

(c)

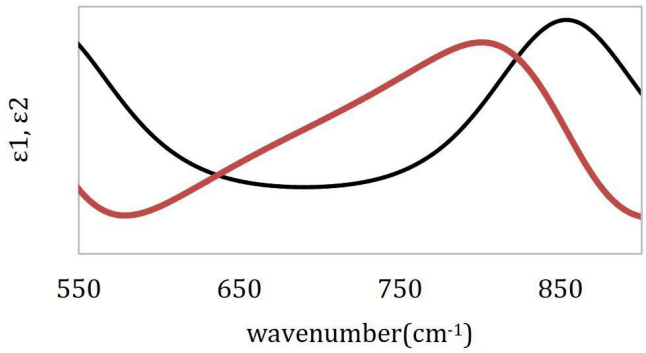

(d)

Figure 4. The values of real dielectric function (ε_1) and imaginary dielectric function (ε_2) in $LiTaO_3$ films doped with Iron Oxide are as follows: (a) 0%, (b) 2%, (c) 4%, and (d) 6%.

Based on Figure 4, the values of ε_1 and ε_2 are obtained, as indicated in Table 3.

Table 3 The value of ε_1 intersects with ε_2 in the thin $LiTaO_3$ film doped with Iron Oxide

Iron Oxide (%)	$\varepsilon 1$ intersects $\varepsilon 2$
0	515
2	485
4	520
6	625

Table 3 presents the values of ε_1 intersecting with ε_2 in the Iron Oxide doped $LiTaO_3$ Thin Films based on Figure 4. As the percentage of Iron Oxide dopant added to the $LiTaO_3$ thin film increases, there is a tendency for the values of ε_1 to intersect with ε_2 to become larger. Similarly, with the real refractive index (n) and imaginary refractive index (k), this result is presumed to be due to the increase in reflectance values as shown in Figure 2.

The intersections of ε_1 and ε_2 are associated with conditions when $\varepsilon_1 = 0$ and $\varepsilon_2 \neq 0$, indicating the decay of electromagnetic waves that are related to optical phonons. (Note that these intersections are related to the $\varepsilon_1 = 0$ and $\varepsilon_2 \neq 0$ conditions, indicating the decay of electromagnetic waves associated with optical phonons. FTIR ATR devices electric field are set from 0° until 180° causes the values of TO, LO, ε_1 and ε_2 diferent to add Ion Oxide doped to $LiTaO_3$ thin film). Figure 3 also demonstrates that the real and imaginary dielectric function graphs have a phase difference of 180°. The dielectric function of the real (ε_1) and imaginary (ε_2) parts have a phase difference of 180°.

4. CONCLUSION

By analyzing the optical-phonon parameters of TO and LO, we have successfully characterized the features of $LiTaO_3$ thin film doped with Fe_2O_3. We have determined that the TO and LO are affected non-monotonously by the variation of Fe_2O_3 doping, which was determined by studying the optical-phonon wavelengths. FTIR ATR devices electric field are set from 0° until 180° causes the values of TO, LO, ε_1 and ε_2 diferent to add Ion Oxide doped to $LiTaO_3$ thin film. Based on the analyses of TO, LO, ε_1 and ε_2, film fabrication of $LiTaO_3$ has the potential as light, pressure and temperature sensors.

ACKNOWLEDGEMENTS

The research study was funded by the Hibah Penelitian Terapan Kompetitif Nasional (PTKN), Direktorat Jendral Pendidikan Tinggi, Riset dan Teknologi, Kementerian Pendidikan, Kebudayaan, Riset dan Teknologi, Republic of Indonesia under contract: 001/E5/PG.02.00.PL/2023.

REFERENCES

[1] Beata Zielińska, Ewa Mijowska, & Ryszard J. Kalenczuk. Materials Characterization, vol 68, 2012 pp. 71-76.
[2] Haribabu Palneedi, Mahesh Peddigari, Ashutosh Upadhyay, José P.B. Silva, Geon-Tae Hwang, & Jungho Ryu. Ferroelectric Materials for Energy Harvesting and Storage. (2022) pp. 279- 356.
[3] AhmadSafari, E. KorayAkdoğan, & Jack D. Leber. Japanese Journal of Applied Physics. Vol 61, (2022).
[4] Li Chen, Mei Er Pam, Sifan Li, & Kah-Wee Ang. Neuromorphic Computing and Engineering. Vol 2, issue 2 (2022).
[5] Alejandra Hortencia Miranda González, Alexandre Z Simões, Maria Aparecida Zaghete, & Jose A. VarelaJose A. Varela. Materials Characterization. vol 50, (2003) pp. 233-238.
[6] Yong-Jin Seo & Sung-Woo Park. The Korean Physical Society. vol 45, issue 3 (2004), pp. 769-772.
[7] Salim Mustofa & Saeful Yusuf. Indonesian Journal of Materials Science. vol 14, issue 4 (2013) pp, 290 – 294.
[8] Tomohiko Nakajima, Tetsuo Tsuchiya, Masaki Ichihara, Hideaki Nagai, & Toshiya Kumagai. Chem. Mater. 2008, vol 20, (2008) pp. 7344–7351.
[9] Mridula Biswas & Pei-Chen Su. Chapter Metrics Overview. (2017).
[10] Irzaman, Ridwan Siskandar, Nida Nabilah, Aminullah, Brian Yuliarto, Kholoud Ahmed Hamam & Husin Alatas. Ferroelectrics. vol 524(2018), pp. 44-55.
[11] Irzaman, Dezya Salsabila Prawira, Irmansyah, Brian Yuliarto & Ulfah Juniarti Siregar. Integrated Ferroelectrics. vol 201 (2019), pp. 32-42.
[12] Reza Zamiri, Hossein Mahmoudi Chenari, H. F. Moafi, Mehdi Shabani, S. A. Salehizadeh f, Avito Rebelo, J. Suresh Kumar, M. P. F. Graça, M. J. Soares , & J. M. F. Ferreira. Ceramics International. vol 42, Issue 11 (2016), pp. 12860-12867.
[13] Dahlang Tahir, Sultan Ilyas, Roni Rahmat, Heryanto Heryanto, Ahmad Nurul Fahri, Mufti Hatur Rahmi, Bualkar Abdullah, Chol Chae Hong, & Hee Jae Kang. ACS Omega. vol 6, (2021) pp. 28334-28346.
[14] Yang Li, Wenlan Qiu, Fan Qin, Hui Fang, Viktor G. Hadjiev, Dmitri Litvinov, & Jiming Bao. J. Phys. Chem, vol 120, issue 8 (2016) pp. 4511–4516.